 Letter

Optics Letters

Compact, widely tunable ultrashort burst pulse generator using four mirrors

RIKAKO TANAKA,[1,†] KEITARO SHIMADA,[1,†] AYUMU ISHIJIMA,[2,*] ETSUKO KOBAYASHI,[1] HIDEHARU MIKAMI,[2] ICHIRO SAKUMA,[1,3] AND KEIICHI NAKAGAWA[1]

[1]Graduate School of Engineering, The University of Tokyo, Tokyo 113-8656, Japan
[2]Research Institute for Electronic Science, Hokkaido University, Hokkaido, 001-0021, Japan
[3]Medical Device Development and Regulation Research Center, The University of Tokyo, Tokyo 113-8656, Japan
[†]These authors contributed equally to this work.
*ishijima@es.hokudai.ac.jp

Received 29 January 2025; revised 23 March 2025; accepted 13 April 2025; posted 14 April 2025; published 24 April 2025

Ultrashort burst laser pulses serve as powerful tools for precise laser processing, broadband ultrafast spectroscopy, and high-speed laser-scanning microscopy. However, the performance of conventional burst pulse generators is limited by constraints in the pulse time interval variability, pulse energy variability, pulse number variability, and overall system complexity. Here, we present a compact burst pulse generator that offers a broad tuning range for pulse time intervals, along with control over the number of pulses and pulse energies within the burst. It consists of four mirrors, two of which are parallel to each other, and outputs pulses that are equally spaced both temporally and spatially. We demonstrated the generation of a burst laser pulse by shaping a single ultrashort laser pulse into six pulses with time intervals ranging from femtoseconds to nanoseconds. The pulse time intervals and energies were consistent with theoretical results.

https://doi.org/10.1364/OL.557473

Recent advancements in high-power femtosecond (fs) laser sources and pulse-shaping technologies have enabled the generation of high-energy burst laser pulses—packets of high-repetition-rate pulses repeated at lower frequencies—spanning applications in broad research areas and industrial fields [1,2]. For example, in laser processing, the usage of bursts of femtosecond (fs) laser pulses at gigahertz (GHz) frequencies enhances the processing precision and material ejection efficiency compared with single-pulse laser processing [3,4]. In ultrafast spectroscopy, frequency-dependent material responses in the GHz to terahertz (THz) range can be probed using burst laser pulses with tunable temporal spacing [5–7]. Moreover, the use of burst laser pulses increases the data acquisition speed in laser-scanning microscopy, where each pulse is directed toward separate regions of a biological sample for the spatiotemporal multiplexing measurement of fluorescence [8–12]. These successes in various applications of burst laser pulses have led to a growing demand for further technological developments of the method to precisely control the time interval, energy, and number of pulses within a burst.

However, conventional burst pulse generators often lack one or more of the following attributes: wide tunability of the pulse time interval, variability in the energy for each pulse within the burst, variability in the pulse number, and system compactness. The generation of burst laser pulses can be classified into two methods: (1) adjusting the repetition frequency of the seed laser pulse using a pulse picker [e.g., electro-optic modulator (EOM) and acousto-optic modulator (AOM)] before entering the laser amplifier [13,14] and (2) shaping a single amplified fs laser pulse into sub-pulses using a free-space delay line [15–20]. While the former method is widely used in industrial applications such as laser manufacturing, unwanted pulse distortion and optical damage to the gain medium limit control over the pulse time interval, pulse energy, and pulse number. In methods to generate burst laser pulses using a free-space delay line such as Fabry–Perot cavities [15,16], spectrum circuit [17,18], spectrum shuttle [19], free-space angular-chirp-enhanced delay [20], and Deathstar [21–23], the pulse time interval corresponds to the round trip length of circulation or reflection. Hence, its time interval can be easily changed by controlling the position of the optics. However, previous methods require complicated and large optical systems to achieve pulse time intervals of ~10 ps or less, posing challenges for system integration. Additionally, large optical systems inherently increase the optical path length, which reduces their robustness to environmental disturbances such as vibrations and air turbulence.

In this Letter, we present a dual parallel reflection (DPR) burst pulse generator that provides a wide tuning range for the pulse time interval while allowing for control of the pulse energy and pulse number. It consists of four mirrors, two of which are parallel to each other, and outputs pulses that are equally spaced both temporally and spatially (Fig. 1). The first set of mirrors consists of a reflective mirror (mirror 1 in Fig. 1) and a partially reflective mirror (mirror 2 in Fig. 1), each with a rotation angle around the y axis. The second set of mirrors consists of two reflective mirrors (mirrors 3 and 4 in Fig. 1), each with a rotation angle around the x and y axes. After passing through the first set of mirrors, the pulses are aligned parallel to the horizontal

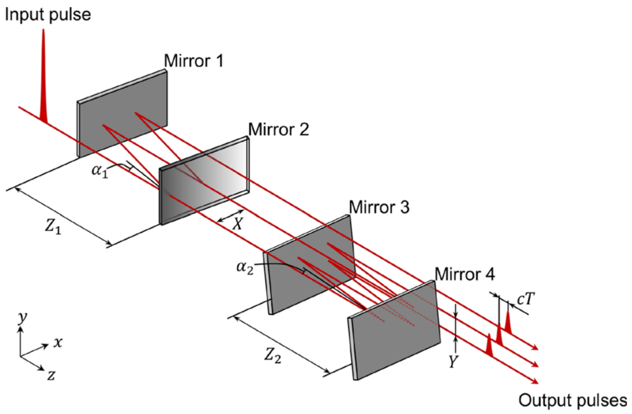

Fig. 1. Schematic of a DPR burst pulse generator with three output pulses. Mirrors 1 and 2 and mirrors 3 and 4 are parallel to each other. The dashed lines indicate rays obscured by mirror 4.

direction and pass through the upper part of mirror 3. Thereafter, the pulses are reflected by mirror 4 and undergo multiple reflections in the second set of mirrors. The pulses incident on the second set of mirrors are reflected different number of times, resulting in a final output of pulses that are equally aligned in the vertical direction. Consequently, the incident single pulses are repeatedly reflected and transmitted in the parallel set of mirrors, producing temporally and spatially equally spaced pulses.

We can widely tune the pulse time interval by changing the distance between the second set of mirrors. The time interval of the pulse T is expressed as

$$T = \frac{\left(Z_2 + \sqrt{{Z_2}^2 - X^2 - Y^2}\right) - \left(Z_1 + \sqrt{{Z_1}^2 - X^2}\right)}{c}, \tag{1}$$

where c is the speed of light, X is the spatial distance between adjacent pulses after passing through the first set of mirrors, Y is the spatial distance between adjacent pulses after passing through the second set of mirrors, Z_1 is the distance between the first set of mirrors in the z-direction $[Z_1 > (2X^2 + Y^2)/\left(2\sqrt{X^2 + Y^2}\right)]$, and Z_2 is the distance between the second set of mirrors in the z-direction $({Z_2}^2 > X^2 + Y^2)$. Equation (1) (see Supplement 1 for the derivation of the equation) is valid for $0 < \alpha_1 \leq \pi/4$ and $0 < \alpha_2 \leq \pi/4$, where α_1 and α_2 are the angles of incidence of the pulses on the first and second set of mirrors, respectively. The time delay produced by the first set of mirrors is canceled by the second set of mirrors at $Z_2 = Z_2'$, where Z_2' is expressed as

$$Z_2' = \frac{X^2 + Y^2 + \left(Z_1 + \sqrt{{Z_1}^2 - X^2}\right)^2}{2\left(Z_1 + \sqrt{{Z_1}^2 - X^2}\right)}. \tag{2}$$

There is a linear relationship between the pulse time interval and the distance between the second set of mirrors in the z-direction when ${Z_2}^2 \gg X^2 + Y^2$ (Fig. 2). Moreover, without using the second set of mirrors, it is difficult to output a burst laser pulse with an fs-order pulse time interval for an input beam diameter larger than a few millimeters and an output number of pulses greater than three (see Supplement 1, Fig. S2).

The energy of each pulse within the burst can be controlled by changing the reflectance and transmittance of the partially

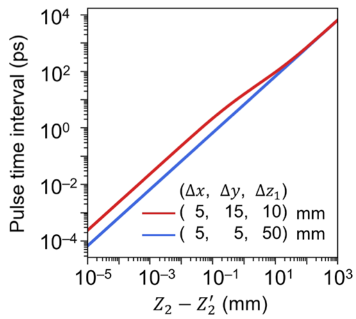

Fig. 2. Theoretical plot of the pulse time interval with the distance between the second set of mirrors in the z-direction. The offset on the distance between the second set of mirrors (Z_2') is subtracted on the horizontal axis.

reflective mirror (mirror 2 in Fig. 1). The transmittance profile of a partially reflective mirror is expressed as

$$T_i = \frac{I_i}{(1 - r\prime) I_0 r^{2M-i-1} \prod_{k=1}^{i-1} R_k}, \tag{3}$$

where i is an integer denoting the pulse number ($i = 1$ denotes the pulse transmitted first through the partially reflective mirror), I_i is the pulse energy after passing through the second mirror, $r\prime$ is the reflectance on the back side of the partially reflective mirror (mirror 2 in Fig. 1), r is the reflectance of the reflective mirror (mirrors 1, 3, and 4 in Fig. 1), M is the total number of output pulses, and R_i is the reflectance of the partially reflective mirror in the region traversed by the i-th pulse (see Supplement 1 for the derivation of the equation). By designing a partially reflective mirror with the transmittance profile based on Eq. (3), the desired energy for each pulse within the burst is obtained. Figure 3(a) shows the pulse energy of the burst laser pulse for output pulses of 20 ($M = 20$). For the calculations, the energy losses from the DPR burst pulse generator were neglected ($r = 1$, $r' = 0$, and $I_0 = \sum_{k=1}^{M} I_k$). Three different transmittance profiles of the partially reflective mirror were assumed in the calculations [Fig. 3(b)]. The DPR burst pulse generator enables tailoring burst laser pulses with various temporal patterns by designing the transmittance profile of a partially reflective mirror. Noted that as shown in Fig. 3(b), it is impossible to completely match the total energy of the burst laser pulse to the pulse energy entering the DPR burst pulse generator ($I_0 > \sum_{k=1}^{M} I_k$) because finite sections of the Gaussian distribution are discretized to produce a Gaussian-distributed burst pulse. Therefore, unlike the other transmittance profiles of the partially reflective mirrors, the transmittance in the area through which the 20th pulse passed did not reach 100%.

To evaluate the performance of the DPR burst pulse generator, we constructed it in a 100 mm × 500 mm space. To the best of our knowledge, its size is more compact than previous methods [21–23] with a comparable pulse time interval tuning range (see Supplement 1). As a proof-of-principle experimental setup, we used a step-density filter (32-599, Edmund) as a partially reflective mirror to produce six pulses. The distance between the first set of mirrors was set to $Z_1 = 46.8$ mm, and the spatial distance between adjacent pulses after passing through the first set of mirrors was set to $X = 4.6$ mm. The spatial distance between the adjacent pulses after passing through the second set of mirrors was set to $Y = 3.2$ mm. A mode-locked Ti:sapphire laser with

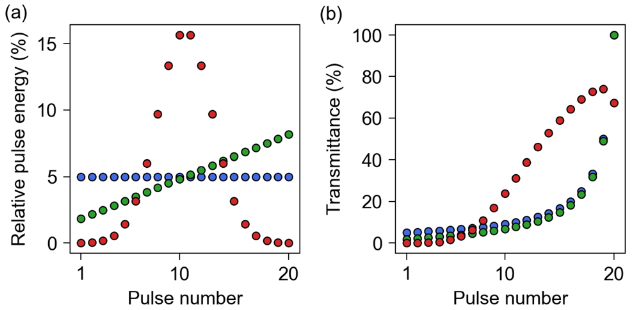

Fig. 3. Theoretical plots of the pulse energy for each pulse within the burst. (a) Output pulse energy distribution for a pulse number of 20 (red, Gaussian; green, linear increase; blue, constant). (b) Transmittance profile of a partially reflective mirror to produce the output pulse energy distribution shown in (a). The correspondence between the output pulse energy distribution and transmittance profile is shown in the same color plots.

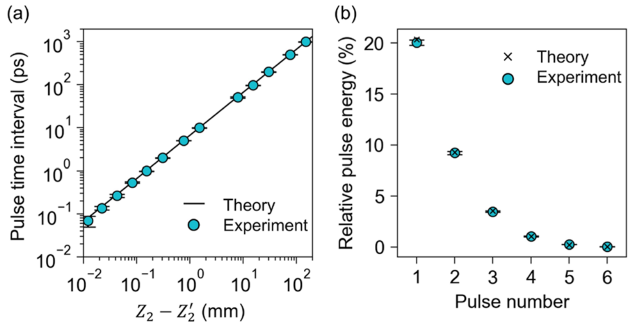

Fig. 4. Producing GHz to THz burst laser pulses by a DPR burst pulse generator. (a) Pulse time intervals ranging from 70 ± 20 fs to 1.000 ± 0.003 ns adjusted by the distance between the second set of mirrors in the z-direction. The error bar represents the standard deviation of the pulse intervals among six pulses. (b) Energy for each pulse within the burst. The error bar represents the standard deviation of the energy for 60,000 pulses.

a chirped pulse amplifier system (Astrella-USP-1 K, Coherent) was used as the light source to generate an ultrashort pulse laser with a central wavelength of 803 nm, a bandwidth of 35 nm, and a pulse width of 35 fs at a repetition rate of 1 kHz.

We first demonstrated the generation of burst laser pulses with pulse time intervals ranging from femtoseconds to nanoseconds. The pulse time interval was changed by adjusting the distance between the second set of mirrors in the z-direction while maintaining the spatial distance between adjacent pulses. The time intervals of pulses exceeding sub-nanoseconds were measured using a 33-GHz photodiode (DPO7OE1, Tektronix) with a 23-GHz oscilloscope (MSO72304DX, Tektronix). The time intervals of pulses of picoseconds or less were measured using cross correlation. For cross correlation measurements, the pulse was split using a beam splitter before entering the DPR burst pulse generator to create a reference pulse. A delay line was placed in the reference beam path. The burst laser pulse and reference pulse were focused onto a beta barium borate crystal (5 mm × 5 mm × 2 mm) using a lens. A frequency-doubled laser pulse was detected using a photodiode (DET36A/M, Thorlabs) connected to an oscilloscope. The measured pulse intervals agreed with the theoretical curves calculated using Eq. (1) [Fig. 4(a); see Supplement 1].

Next, the energy of each pulse within a burst was measured. The theoretical values were calculated by substituting the transmittance and reflectance of the partially reflective mirror into Eq. (3). The pulse energy was measured using an energy meter (PM100D, Thorlabs). As shown in Fig. 4(b), the measured energy of the pulses reflects the transmittance profile of the partially reflective mirror. These results indicate that the energy of each pulse within the burst can be controlled by the transmittance profile of the partially reflective mirror. Therefore, it is important to select a substrate of partially reflective mirror with negligible absorption for minimizing laser power loss by the DPR burst pulse generator.

We next compare the DPR burst pulse generator with previous burst pulse generators. First, the DPR burst pulse generator uses fewer optical elements and requires a shorter optical path length compared to Deathstar [21–23], which has a similar tunable range of the pulse time interval, pulse energy, and pulse number within the burst (see Supplement 1). Using fewer optical elements minimizes error accumulation from mirror flatness and surface roughness, while a shorter optical path length enhances robustness against environmental disturbances such as vibrations and air turbulence. However, the DPR burst pulse generator requires an adjustment of the mirror angle in addition to changing the spacing of the second set of mirrors to change the pulse time interval. Regarding pulse energy tunability, similar to its use in Deathstar, the partially reflective mirror of the DPR burst pulse generator needs to be replaced with specifically designed one to achieve the desired energy distribution for each application. Second, the DPR burst pulse generator outputs pulses that are equally spaced both temporally and spatially, whereas other burst generators such as the reverberation loop [9], Fabry–Perot cavities [15,16], spectrum circuits [17,18], and spectrum shuttle [19] output collinear burst laser pulses. As a result, the full aperture of the objective lens cannot be utilized to focus the burst laser pulses on the sample. However, our method offers advantages in situations where burst laser pulses are focused with a low numerical aperture condition in applications such as laser processing, laser-scanning microscopy, and phonon spectroscopy. Although the DPR burst pulse generator can output collinear burst laser pulses by placing a retro-reflecting mirror immediately after the second set of mirrors, such an approach results in a power loss.

The DPR burst pulse generator is expected to have a wide range of scientific and industrial applications. Because it can generate burst laser pulses at fs time intervals, it can be used as a burst generator for single-shot ultrafast spectroscopy [24,25] and THz burst-mode laser processing [26,27]. Furthermore, the use of burst laser pulses to generate multi-cycle longitudinal waves can potentially enhance the acoustic signal from biological samples and increase the signal-to-noise ratio [5,21]. Therefore, the ability to generate burst laser pulses on sub-nanosecond timescales enables the possibility of using the DPR burst pulse generator in phonon spectroscopy to study cell biomechanics, where the Brillouin frequency of biological cells is typically on the order of ∼1 GHz [28–30].

In conclusion, we presented an ultrashort burst pulse generator that provides a wide tunable range of pulse time intervals while allowing control of the pulse number and pulse energy. The generation of burst laser pulses was demonstrated by shaping a single femtosecond laser pulse into six pulses with pulse intervals ranging from femtoseconds to nanoseconds, closely matching their pulse time intervals and energies with theoretical results. Our simple and compact burst pulse generator has the potential to replace conventional non-collinear burst pulse generators, enabling precise control of the pulse time interval, pulse number, and pulse energy.

Funding. Japan Science and Technology Agency (JPMJPR1902); Japan Society for the Promotion of Science (23K18584); Basic Research Program of the Network Joint Research Center for Materials and Devices; Murata Science and Education Foundation; Sumitomo Foundation.

Acknowledgment. We thank Takao Saiki for fruitful discussions.

Disclosures. The authors declare no conflicts of interest.

Data availability. Data underlying the results presented in this Letter are available from the corresponding author upon reasonable request.

Supplemental document. See Supplement 1 for supporting content.

REFERENCES

1. L. Jiang, A.-D. Wang, B. Li, *et al.*, Light: Sci. Appl. **7**, 17134 (2018).
2. J. Wu, N. Ji, and K. K. Tsia, Nat. Photonics **15**, 800 (2021).
3. M. Park, Y. Gu, X. Mao, *et al.*, Sci. Adv. **9**, eadf6397 (2023).
4. C. Kerse, H. Kalaycıoĝlu, P. Elahi, *et al.*, Nature **537**, 84 (2016).
5. T. Pezeril, C. Klieber, S. Andrieu, *et al.*, Phys. Rev. Lett. **102**, 107402 (2009).
6. A. Bojahr, M. Gohlke, W. Leitenberger, *et al.*, Phys. Rev. Lett. **115**, 195502 (2015).
7. A. Bojahr, M. Herzog, S. Mitzscherling, *et al.*, Opt. Express **21**, 21188 (2013).
8. S. Weisenburger, F. Tejera, J. Demas, *et al.*, Cell **177**, 1050 (2019).
9. D. R. Beaulieu, I. G. Davison, K. Kılıç, *et al.*, Nat. Methods **17**, 283 (2020).
10. J. Demas, J. Manley, F. Tejera, *et al.*, Nat. Methods **18**, 1103 (2021).
11. J. Platisa, X. Ye, A. M. Ahrens, *et al.*, Nat. Methods **20**, 1095 (2023).
12. B. Li, C. Wu, M. Wang, *et al.*, Nat. Methods **17**, 163 (2020).
13. Y. Liu, J. Wu, X. Wen, *et al.*, Opt. Express **28**, 13414 (2020).
14. T. Bartulevicius, M. Lipnickas, V. Petrauskiene, *et al.*, Opt. Express **30**, 36849 (2022).
15. L. Dresselhaus-Cooper, J. E. Gorfain, C. T. Key, *et al.*, Sci. Rep. **9**, 3689 (2019).
16. A. Okhrimchuk, S. Fedotov, I. Glebov, *et al.*, Sci. Rep. **7**, 16563 (2017).
17. T. Saiki, K. Shimada, A. Ishijima, *et al.*, Sci. Adv. **9**, eadj8608 (2023).
18. T. Saiki, A. Ishijima, I. Sakuma, *et al.*, in *2020 Conference on Lasers and Electro-Optics (CLEO)* (IEEE, 2020), pp. 1–2.
19. K. Shimada, A. Ishijima, T. Saiki, *et al.*, Adv. Photonics Nexus **3**, 016002 (2024).
20. J.-L. Wu, Y.-Q. Xu, J.-J. Xu, *et al.*, Light: Sci. Appl. **6**, e16196 (2017).
21. J. D. Choi, T. Feurer, M. Yamaguchi, *et al.*, Appl. Phys. Lett. **87**, 081907 (2005).
22. C. Klieber, E. Peronne, K. Katayama, *et al.*, Appl. Phys. Lett. **98**, 211908 (2011).
23. Y. Kai, J. Lem, M. Ossiander, *et al.*, Opt. Express **31**, 31308 (2023).
24. P. R. Poulin and K. A. Nelson, Science **313**, 1756 (2006).
25. S. W. Teitelbaum, T. Shin, J. W. Wolfson, *et al.*, Phys. Rev. X **8**, 031081 (2018).
26. C. Gaudiuso, P. N. Terekhin, A. Volpe, *et al.*, Sci. Rep. **11**, 13321 (2021).
27. J. Mur and R. Petkovšek, Appl. Surf. Sci. **478**, 355 (2019).
28. A. Ishijima, S. Okabe, I. Sakuma, *et al.*, Photoacoustics **29**, 100447 (2023).
29. B. Audoin, Photoacoustics **31**, 100496 (2023).
30. F. Pérez-Cota, R. Fuentes-Domínguez, S. La Cavera, *et al.*, J. Appl. Phys. **128**, 160902 (2020).